Blind OFDM Channel Estimation Through Simple Linear Precoding

Athina Petropulu, Ruifeng Zhang, *Member, IEEE*, and Rui Lin

***Abstract*—A novel approach of blind channel estimation for orthogonal frequency-division multiplexing (OFDM) systems is proposed. A linear transformation is applied on each block before it enters the OFDM system. The transform imposes a correlation structure on the transmitted blocks, which is exploited at the receiver to recover the channel via simple cross-correlation operations. The proposed approach is computationally simple and converges fast, which makes it a good candidate for estimation of fast-varying channels. Its performance is tested analytically, through a mean-square error analysis, and also via simulations. Results show that it compares favorably to the training-based scheme used in the IEEE 802.11a wireless standard.**

***Index Terms*—Blind channel estimation, orthogonal frequency-division multiplexing (OFDM) systems, precoding.**

I. Introduction

It IS well understood that the communication channel sets a limit to the transmission rate of the communication system. Signal pulses are broadened in time as they travel through the channel (multipath effect), leading to intersymbol interference (ISI). The pulse spread limits the speed at which adjacent data pulses can be sent without overlap, thus limiting the maximum information rate of the wireless system. One technique to avoid the effect of multipath, without sacrificing the transmission rate, is multicarrier modulation [29]. This is a parallel transmission scheme, where the overall frequency band is divided into a number of subbands with separate subcarriers. On each subcarrier, the modulated symbol rate is low in comparison to the channel delay spread, thus ISI can be prevented. An increasingly popular multicarrier modulation technique is orthogonal frequency division multiplexing (OFDM) [6], [9], [13]. It has been implemented in several wireline and wireless high-speed data communications standards (ADSL [1], IEEE 802.11 [5], HiperLAN [2]) and has been adopted by the European digital audio and video broadcasting standards (DAB [4] and DVB [3]).

OFDM modulation is performed using the following steps. First, the information-bearing symbol, modulated via any type of constellation (e.g., BPSK, QAM) is segmented into blocks of length N. An N-point inverse discrete Fourier transform (IDFT) is then performed on each block, and a preamble, consisting of the last N_{cp} IDFT samples, called cyclic prefix (CP), is appended in front of the IDFT block. The augmented blocks are sent one after the other through the communications channel. As long as the channel length is smaller than the length of the cyclic prefix, the spreading of the block, caused by the convolution with the channel, affects less than N_{cp} symbols. Thus, interference occurs between two adjacent blocks only. At the receiver, the cyclic prefix part is discarded, and an N-point DFT is performed on the remaining N-symbol segment of the block. It can be shown that the received symbol at the kth carrier equals the transmitted one scaled by the channel frequency response at frequency k. Thus, multicarrier modulation armed with a cyclic prefix effectively turns the wideband frequency-selective channel into a number of parallel narrowband frequency-flat subchannels.

Although ISI can be avoided, via the use of cyclic prefix, the phase and gain of each subchannel is needed for coherent symbol detection. An estimate of these parameters can be obtained with pilot/training symbols [8], [14], [19], [20], [26], at the expense of bandwidth. Blind channel estimation methods avoid the use of pilot symbols, which makes them good candidates for achieving high spectral efficiency. Existing blind channel estimation methods for OFDM systems can be classified as statistical and deterministic. The statistical methods explore the cylcostationarity that the cyclic prefix induces to the transmitted signal. They recover the channel using cyclic statistics of the received signal [16] or subspace decomposition of the correlation matrix of the pre-DFT received blocks [11], [27], [32]. The deterministic methods process the post DFT received blocks and exploit the finite-alphabet property of the information-bearing symbols. A maximum likelihood approach has been proposed in [12], and iterative Bayesian methods that alternate between channel estimation and symbol detection/decoding have been proposed in [22], [24], and [30] for the case of coded OFDM systems. Taking into account specific properties of M-PSK or QAM signals while utilizing an exhaustive search, a blind method has been proposed in [31]. In comparison to the statistical methods, the deterministic ones converge much faster; however, they involve high complexity, which becomes even higher as the constellation order increases. A deterministic blind channel estimation method that takes advantage of receive diversity and does not require an exhaustive search has been proposed in [28]. Receive diversity has also been proposed for blind channel estimation in OFDM systems without cyclic prefix in [7] and [18].

In this paper, we propose an approach that belongs to the statistical class. It consists of a simple linear transformation

Manuscript received July 9, 2002; revised December 6, 2002 and March 20, 2003; accepted March 21, 2003. The editor coordinating the review of this paper and approving it for publication is G. Leus. This work was supported by the ONR under Grant N00014-03-1-0123.

The authors are with the Department of Electrical and Computer Engineering, Drexel University, Philadelphia, PA 19104 USA (e-mail: athina@ece.drexel.edu).

Digital Object Identifier 10.1109/TWC.2003.821140

applied to blocks of symbols before they enter the OFDM system, which enables blind channel estimation at the output of the OFDM system via cross-correlation operations. Unlike other coded OFDM schemes [10], [22]–[25], [30], the proposed one does not introduce redundancy to the block, nor does it change the block length. The proposed channel estimation method is computationally simpler than deterministic methods and subspace approaches.

The paper is organized as follows. Section II specifies the proposed OFDM system and Section III presents the proposed blind channel estimation method. Section IV provides analytic expressions for the normalized mean-squared error of the channel estimates, which were obtained based on the proposed approach. Section V includes simulation results that test the performance of the proposed approach and also compares it to the subspace approach of [27]. Finally, concluding remarks are presented in Section VI.

II. Signal Precoding

Let us consider an OFDM system and apply at its input a linear precoding block that performs the following task. It transforms the ith OFDM block of N information symbols $\{d_{i,k}, k = 0, \ldots, N-1\}$ according to

$$s_{i,k} = \frac{1}{\sqrt{1+|A|^2}}(d_{i,k} + (-1)^k A d_{i,T}), \quad k = 0, \ldots, N-1 \tag{1}$$

where T and A are both predefined numbers, assumed to be known to the transmitter and receiver, T is an integer in $[0, N-1]$, and A is a pure imaginary number with $|A| < 1$. This precoding has several properties.

1) It introduces no redundancy to the transmitted data, which makes the approach bandwidth efficient.
2) It preserves the transmission power on each subcarrier. We should note here that the requirement for A to be pure imaginary is necessary in order to maintain the power of the Tth carrier.
3) It maintains the zero-mean of the signal transmitted on each subcarrier.
4) It maintains zero DC offset in each block.
5) It introduces a correlation structure in signals transmitted over different subcarriers, which can be explored for channel estimation.

The coded block $\{s_{i,k}, k = 0, \ldots, N-1\}$ goes through the regular OFDM transmission steps. The ith received OFDM block after removal of the CP and DFT is

$$\begin{aligned} y_{i,k} &= H(k)s_{i,k} + v_{i,k} \\ &= \frac{1}{\sqrt{1+|A|^2}} H(k)(d_{i,k} + (-1)^k A d_{i,T}) + v_{i,k}, \\ k &= 0, \ldots, N-1 \end{aligned} \tag{2}$$

where $H(k)$ is the complex gain of the kth subcarrier, and $v_{i,k}$ models the noise. In the following discussions, we will assume that: 1) the baud-rate channel can be modeled as a finite impulse response (FIR) filter of length L with tap coefficients $h(l)$, $l = 0, \ldots, L-1$; hence, $H(k) = \sum_{l=0}^{L-1} h(l) e^{-j(2\pi/N)kl}$, $k = 0, \ldots, N-1$; 2) the channel stays the same for at least the duration of the block, and is quasistationary between blocks; and 3) the noise $v_{i,k}$ is complex, circular Gaussian, zero-mean, σ_v^2 variance, white across subcarriers and blocks, and independent of the information symbols.

The channel frequency response $H(k), k = 0, \ldots, N-1$, or equivalently, the channel impulse response $h(l), l = 0, \ldots, L-1$, is needed in order to recover the transmitted signal $s_{i,k}$; consequently, the information symbols $d_{i,k}$, $k = 0, \ldots, N-1$. In Section III, it is shown how the correlation structure introduced by the proposed precoding facilitates blind channel estimation.

III. Blind Channel Estimation

Consider the correlation of the signals on the kth and Tth subcarriers, as in (3), shown at the bottom of the page, where σ_d^2 is the variance of the information symbols, and the expectation is taken over successive OFDM blocks. Based on (3), an estimate of the channel $H(k)$ within the complex constant $\sigma_d^2 H^*(T)$, can be obtained as in (4), shown at the bottom of the page. Since A is known to the receiver, the required scaling in (4) is feasible.

The channel estimate of (4) can be further improved, noting that $\hat{H}(k), k = 0, \ldots, N-1$ should be the DFT of the channel impulse response $h(l), l = 0, \ldots, L-1$, where $L < N$. The latter length constraint can be enforced by performing IDFT on $\hat{H}(k)$, setting to zero the last $N-L$ samples of the IDFT output, then performing an N-point DFT on the result. This procedure is referred to as *denoising* [8], and the improved channel estimate equals

$$\begin{aligned} \hat{H}_o(k) &= \frac{1}{N} \sum_{l=0}^{L-1} \sum_{n=0}^{N-1} \hat{H}(n) e^{j(2\pi/N)\ln} e^{-j(2\pi/N)kl}, \\ k &= 0, \ldots, N-1. \end{aligned} \tag{5}$$

$$\begin{aligned} z_{k,T} &\triangleq \mathrm{E}[y_{i,k} y_{i,T}^*] \\ &= \begin{cases} \frac{(-1)^k A + (-1)^{k+T}|A|^2}{1+|A|^2} \sigma_d^2 H^*(T) H(k), & k = 0, \ldots, N-1, \quad k \neq T, \\ \sigma_d^2 H^*(T) H^(T) + \sigma_v^2, & k = T \end{cases} \end{aligned} \tag{3}$$

$$\hat{H}(k) \triangleq \begin{cases} \frac{1+|A|^2}{(-1)^k A + (-1)^{k+T}|A|^2} z_{k,T}, & k = 0, \ldots, N-1, \quad k \neq T, \\ z_{k,T}, & k = T \end{cases} \tag{4}$$

Examining (3) and (4), we can see that $\hat{H}(T)$ is the only sample of the channel response estimate that contains the effect of noise. To eliminate the noise contribution, one could completely discard that sample. There is enough redundancy within the remaining $\hat{H}(k)$s to recover the missing sample, via interpolation, for example.

A potential problem with the estimate of (4) might arise when the Tth carrier is in deep fade, in which case $z_{k,T}$ is close to zero for all ks. However, it is interesting to note that, at the receiver, any subcarrier can play the same role as the Tth one. Let R be an integer in $[0,\ldots,N-1]$ with $R \neq T$. Then we have (6), shown at the bottom of the page. Based on (6), the channel response $H(k)$ can be estimated within the complex constant $\sigma_d^2 H^*(R)$ as

$$\hat{H}(k) \triangleq \begin{cases} \frac{1+|A|^2}{(-1)^{k+R}|A|^2} z_{k,R}, & k \neq R, T \\ z_{k,R}, & k = R, \\ \frac{1+|A|^2}{(-1)^R A^* + (-1)^{T+R}|A|^2} z_{k,R}, & k = T. \end{cases} \tag{7}$$

Although there is no way of knowing in advance what the locations of the channel nulls are, a criterion for selecting R can still be implemented at the receiver. Observing that $H(R)$ scales the amplitude of $z_{k,R}$, R can be selected as

$$R_o = \arg\max_R \sum_{k=0}^{N-1} |z_{k,R}|^2. \tag{8}$$

This step would require the estimation of the entire correlation matrix of the received blocks, thus introducing a small increase in complexity.

A. Resolving the Scalar Ambiguity

Scalar ambiguity is common to all blind channel estimation methods. One way to resolve it is using a pilot symbol. In our case, the pilot could be inserted in the block before or after precoding. In the former case, a good place for inserting the pilot would be the Tth location within the block. Then, the $d_{i,T}$ would be the known pilot. An important property of $d_{i,T}$, as defined in (1), was that it varied from block to block, thus maintaining a zero-mean for the symbol transmitted over each carrier. Thus, if $d_{i,T}$ were to be set to some known value, this value would have to be assigned for each i by a pseudo-random number generator. Perfect cooperation between transmitter and receiver would be needed in this case for the synchronization of the pilot sequence.

The pilot could also be placed in the block after precoding. Assuming that one pilot is placed at location P in the precoded block, then we can obtain an estimate of $H(P)$ based on J received blocks as

$$\hat{H}(P) = \frac{1}{J}\sum_{i=1}^{J} \frac{y_{i,P}}{s_{i,P}} \tag{9}$$

where $s_{i,P}$ is the pilot symbol used in block i.

Subsequently, the channel estimate obtained based on (7) can be normalized with respect to $\hat{H}(P)$.

IV. Performance Analysis

The expectation needed in (3) [or (6)] can be implemented as averaging over a finite number of OFDM symbols, i.e.,

$$\hat{z}_{k,T} = \frac{1}{J}\sum_{i=1}^{J} y_{i,k} y_{i,T}^* \tag{10}$$

where J is referred to as the smoothing factor.

We next investigate the effect of finite sample averaging on the performance of the channel estimation. We consider here the case in which the Tth subcarrier is used for the correlation operation at the receiver. The case where the Rth subcarrier is used can be treated similarly. As a performance metric we use the *normalized mean square error* (NMSE), which is defined as

$$\text{NMSE} \triangleq \frac{\sum_{k=0}^{N-1} \left| \frac{\hat{H}_o(k)}{\sigma_d^2 H^*(T)} - H(k) \right|^2}{\sum_{k=0}^{N-1} |H(k)|^2} \tag{11}$$

where $\hat{H}_o(k)$ is the noise-smoothed channel estimate defined in (5). Under the assumptions of independent and identically distributed information symbols and white Gaussian noise, the NMSE can be derived as

$$\begin{aligned} \text{NMSE} = &\frac{1}{J}\left[\frac{L}{N|A|^2}\left(1 - \frac{|H(T)|^2}{\sum_{k=0}^{N-1}|H(k)|^2}\right) + \left(\frac{\psi_4}{\sigma_d^4} - 1\right)\right] + \frac{1}{J(\text{SNR})} \\ &\times \left[\frac{L}{N|H(T)|^2|A|^2}\left(1 - \frac{|H(T)|^2}{\sum_{k=0}^{N-1}|H(k)|^2}\right) + \frac{L(N+N|A|^2-1)}{N|A|^2\sum_{k=0}^{N-1}|H(k)|^2} + \frac{1}{|H(T)|^2}\right] \\ &+ \frac{1}{J(\text{SNR})^2}\frac{L}{N|H(T)|^2\sum_{k=0}^{N-1}|H(k)|^2} \times \left[(N-1)\frac{1}{|A|^2} + N\right] \\ &+ \frac{1}{(\text{SNR})^2}\frac{L}{N|H(T)|^2\sum_{k=0}^{N-1}|H(k)|^2} \end{aligned} \tag{12}$$

$$z_{k,R} \triangleq \text{E}[y_{i,k}y_{i,R}^*] = \begin{cases} \frac{(-1)^{k+R}|A|^2}{1+|A|^2}\sigma_d^2 H^*(R)H(k), & k = 0,\ldots,N-1, \quad k \neq R, \quad k \neq T, \\ \sigma_d^2 H^*(R)H(R) + \sigma_v^2, & k = R\,, \\ \frac{(-1)^R A^* + (-1)^{T+R}|A|^2}{1+|A|^2}\sigma_d^2 H^*(R)H(T), & k = T \end{cases} \tag{6}$$

where $\psi_4 = \mathrm{E}\left[|d_{i,k}|^4\right]$ is the kurtosis of the information symbol and $\mathrm{SNR} = \sigma_d^2/\sigma_v^2$ is the signal-to-noise ratio. The details of the derivation can be found in Appendix A.

The following observations can be drawn from (12).

1) NMSE decreases almost linearly with the SNR and the smoothing factor J.

2) As $\mathrm{SNR} \longrightarrow \infty$,

$$\mathrm{NMSE} \longrightarrow \frac{1}{J}\left[\frac{L}{N|A|^2}\left(1-\frac{|H(T)|^2}{\sum_{k=0}^{N-1}|H(k)|^2}\right)\left(\frac{\psi_4}{\sigma_d^4}-1\right)\right]. \tag{13}$$

As $J \longrightarrow \infty$

$$\mathrm{NMSE} \longrightarrow \frac{1}{(\mathrm{SNR})^2}\frac{L}{N|H(T)|^2\sum_{k=0}^{N-1}|H(k)|^2}. \tag{14}$$

Thus, for NMSE to vanish, both SNR and J should approach infinity. If J is kept small, then as SNR increases the NMSE will level off to some nonzero value. The error floor can be lowered by increasing J.

3) The larger the value of $|A|$, the smaller the NMSE will be. However, the effect of A on bit-error rate (BER) is different. Consider the equalized output for the kth subcarrier

$$\hat{d}_{i,k} = G(k)H(k)d_{i,k} + (-1)^k A(G(k)H(k)-1)d_{i,T} + \sqrt{1+|A|^2}G(k)v_{i,k} \tag{15}$$

where for the MMSE equalizer

$$G(k) = \frac{\hat{H}_o^*(k)}{|\hat{H}_o(k)|^2+\sigma_v^2}. \tag{16}$$

One can see that in case of imperfect channel estimation, A increases intercarrier interference which in turn increases the BER. Therefore, the choice of A should balance out channel estimation error and the bit error rate.

V. Simulation Results

In this section, we present simulation results of the proposed approach. We simulated an OFDM system according to the IEEE 802.11a standard [5], which calls for a block length of $N = 64$ and a cyclic prefix length 8.

The simulated channel was a three-tap ($L = 3$) FIR filter, each tap being independently generated according to the modified Jakes' model [17]. The maximum Doppler frequency normalized with the Nyquist frequency was set to $f_d = 10^{-6}$ and $f_d = 1.5 \times 10^{-4}$. At 5.2-GHz carrier frequency, 54-Mb/s data rate with 64-QAM modulation and 3/4 coding (802.11a standard [5]), $f_d = 10^{-6}$ corresponds roughly to a vehicle speed 0.01 m/s, while $f_d = 1.5\times 10^{-4}$ corresponds to a vehicle speed of 1.5 m/s. The noise was taken as a complex, zero-mean white Gaussian variable with variance σ_v^2.

We simulated N_s OFDM blocks that were transmitted through the time-varying channel. The received blocks were divided into groups of J blocks, where J was selected so that the channel did not change significantly during each J-block segment.

Let $\hat{H}(k; i_0)$ denote the channel estimate obtained based on the i_0th group of received blocks, or, equivalently, the blocks $\{y_{i,k},\ k = 0,\ldots,N-1\}$ corresponding to $i = (i_0-1)J + 1,\ldots,i_0 J$.

For the proposed method, $\hat{H}(k; i_0)$ was obtained based on

$$\hat{z}_{k,R}^{i_0} = \lambda\hat{z}_{k,R}^{i_0-1} + (1-\lambda)\hat{z}_{k,R}^{i_0} \tag{17}$$

where

$$\hat{z}_{k,R}^{i_0} = \frac{1}{J}\sum_{i=(i_0-1)J+1}^{i_0 J} y_{i,k}y_{i,R}^* \tag{18}$$

and λ is a parameter in $[0,1]$. Denoising was implemented according to (5).

The obtained estimate was used to recover the transmitted symbols, $s_{i,k}$, for $i = (i_0-1)J+1,\ldots,i_0+J$, via an MMSE equalizer.

If a pilot is placed at location T of the symbol before precoding, estimates of the symbols are obtained as

$$\hat{d}_{i,k} = \sqrt{1+|A|^2}G(k)y_{i,k} - (-1)^k A d_{i,T}. \tag{19}$$

On the other hand, when a pilot is used after precoding, estimates of the symbols $d_{i,k}$ can be obtained as

$$\hat{d}_{i,k} = \sqrt{1+|A|^2}\left[G(k)y_{i,k} - \frac{(-1)^k A}{1+(-1)^T A}G(T)y_{i,T}\right] \tag{20}$$

where $G(k)$ is the MMSE equalizer as defined in (16). Both of the above described pilots were tested in our simulations but yielded no significant difference in terms of BER performance.

Estimation and symbol recovery for each case considered in the sequel was performed for $M = 50$ Monte Carlo runs, where between runs, independent realizations of noise, input, and channel were used.

The following channel performance metric was used:

$$\mathrm{NMSE}_{i_0} = \frac{1}{M}\sum_{i=1}^{M}\frac{\sum_{k=0}^{N-1}\left[\frac{\alpha}{\hat{H}(T)}\hat{H}^i(k;i_0) - H^i(k;i_0)\right]^2}{\sum_{k=0}^{N-1}[H^i(k;i_0)]^2} \tag{21}$$

where $H^i(k; i_0)$ is the ith realization of the average simulated channel that was experienced by blocks $\{y_{i,k},\ k = 0,\ldots,N-1\}$ corresponding to $(i_0-1)J+1,\ldots,i_0+J$, and α is a normalization parameter, accounting for the scalar ambiguity in the obtained channel estimate. In the following simulations, α was estimated using a pilot symbol placed at the Tth location of each transmitted block after precoding.

Equation (21) can be viewed as the empirical version of the NMSE defined in (11).

As a benchmark, we also tested the performance of the training-based method used in the 802.11a standard, in which

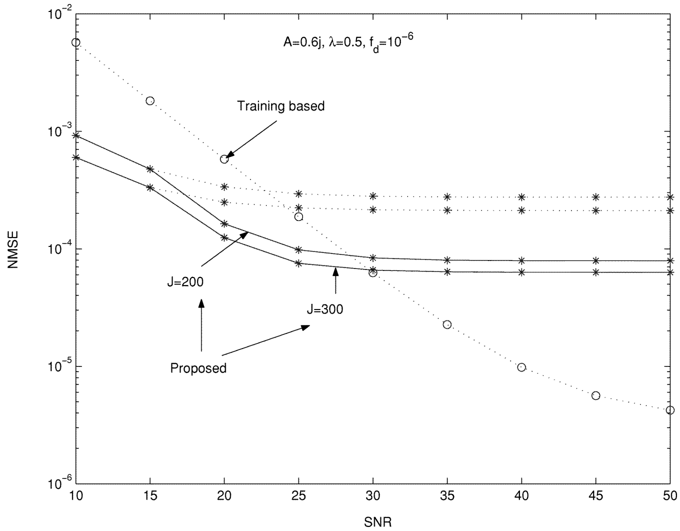

Fig. 1. Slowly varying channel: NMSE of proposed and training-based method. Further reduction of NMSE of the proposed method by combining (23) along with (7) for $\mathrm{SNR} > 15$ dB (solid/star line). Result corresponding to the estimate obtained based on (7) only is shown in dotted/star line.

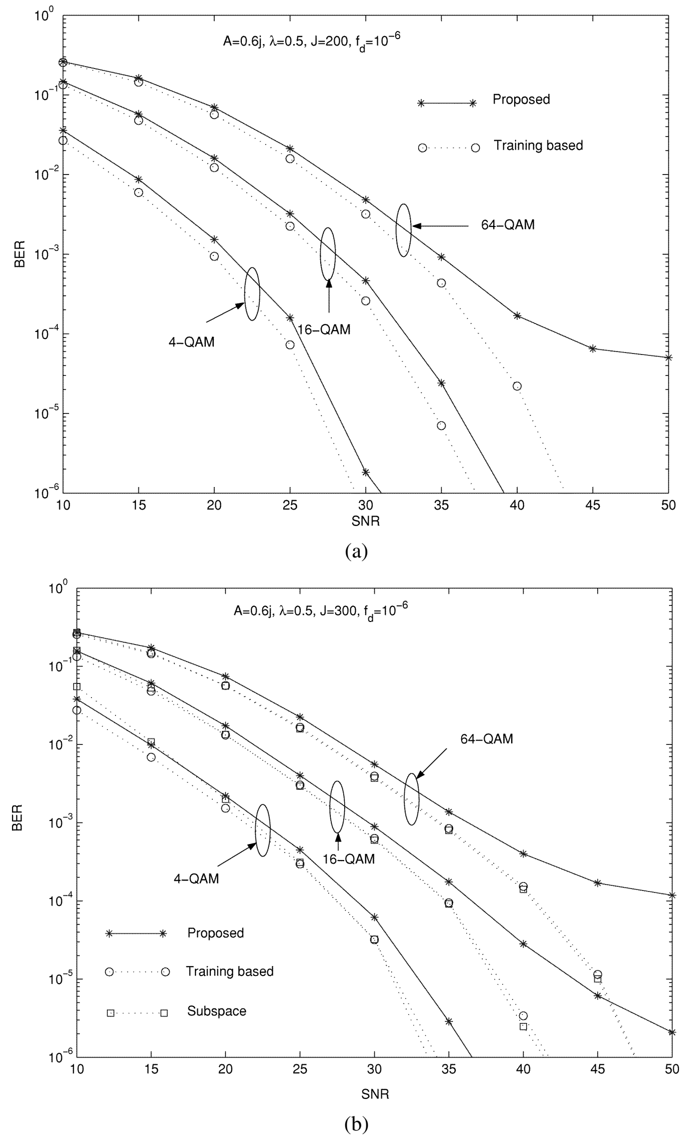

Fig. 2. Slowly varying channel: BER performance of proposed versus training-based and blind subspace method. (a) BER performance for smoothing factor $J = 300$ with minimum channel gain -16.5 dB. (b) BER performance for smoothing factor $J = 300$ with minimum channel gain -20 dB.

the channel is estimated once only, based on two training OFDM blocks, i.e.,

$$\hat{H}_{tr}(k) = \frac{1}{2}\sum_{i=1}^{2}\frac{y_{i,k}}{s_{i,k}}. \quad (22)$$

The obtained channel estimate is then used to recover all N_s transmitted blocks. For a fair comparison, denoising was also implemented for the training-based estimation method.

We also conducted comparisons between the proposed channel estimation method and the blind subspace method proposed in [27]. This approach exploits the redundancy induced to the received data by the cyclic prefix. In particular, the autocorrelation matrix of pairs of received blocks (before cyclic prefix removal) is estimated, and the channel is subsequently computed by exploiting the orthogonality of the signal and noise subspaces of that matrix, through singular value decomposition. The autocorrelation matrix was updated along the lines of (17). Denoising was applied as in the proposed method.

A. Slowly Varying Channel

We first considered the case of a slowly varying channel ($f_d = 10^{-6}$) and simulated transmission of $N_s = 600$ OFDM symbols. Fig. 1 shows the average NMSE obtained with the proposed training-based methods for 64-QAM input signals. The results of the proposed method were obtained with $\lambda = 0.5$, $A = j0.6$, and two different smoothing factors, i.e., $J = 200$ and $J = 300$. One can see that the proposed approach (star dotted lines) achieves lower NMSE than the training-based one for low SNR values. However, while the training-based NMSE continues to drop at higher SNR, the proposed one levels off. The final NMSE level can reduce if the amount of averaging increases. This can be seen by comparing the two sets of curves corresponding to $J = 200$ and $J = 300$.

For high SNR, i.e., higher than 15 db, the NMSE can be further reduced for fixed J. This can be achieved by exploiting additional information available in the autocorrelation of the received signal. An additional channel magnitude estimate can be extracted as follows:

$$|\hat{H}(k)|^2 = \frac{1}{\sigma_d^2} z_{k,k}^i, \quad k = 0, \ldots, N-1. \quad (23)$$

Although $z_{k,k}^i$ contains the effect of noise, at high SNR it produces a better magnitude estimate than (4) or (7). The reduction in NMSE is evident in Fig. 1 (solid/star lines), where for $\mathrm{SNR} \geq 15$ dB, (23) is used along with the phase obtained from (4) or (7) to obtain the channel estimate.

Fig. 2 shows the BER performance of two methods. It can be seen that the proposed method, for this slowly varying channel case, performs comparably to the training-based one. The performance of both methods, however, depends on the level of fading. Fig. 2(a) and (b) shows the performance corresponding to minimum channel gain -16.5 and -20 dB, respectively.

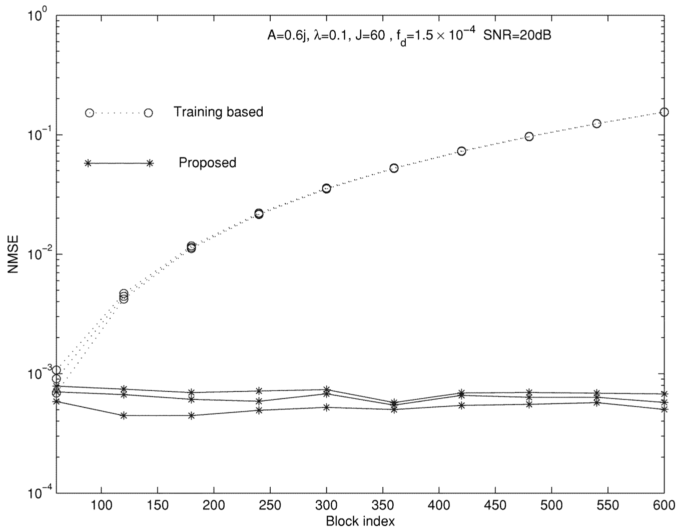

(a)

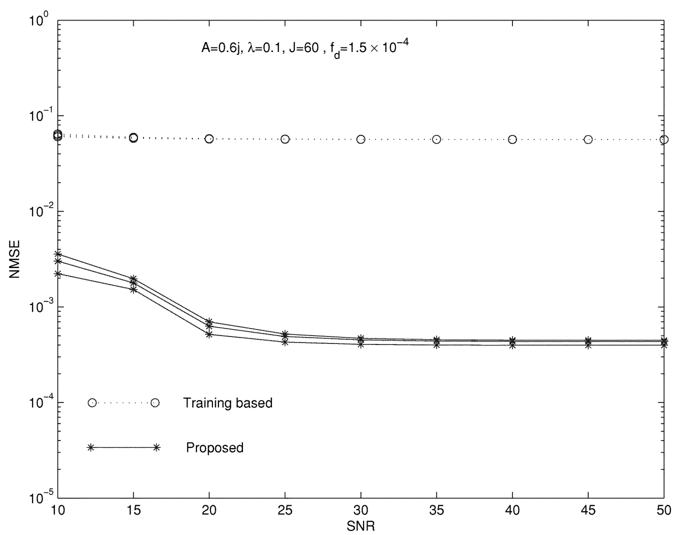

(b)

Fig. 3. Fast varying channel: proposed versus training-based method. (a) Channel estimation error per $J = 100$ blocks at $\mathrm{SNR} = 20$ dB. (b) NMSE of proposed approach and training-based method.

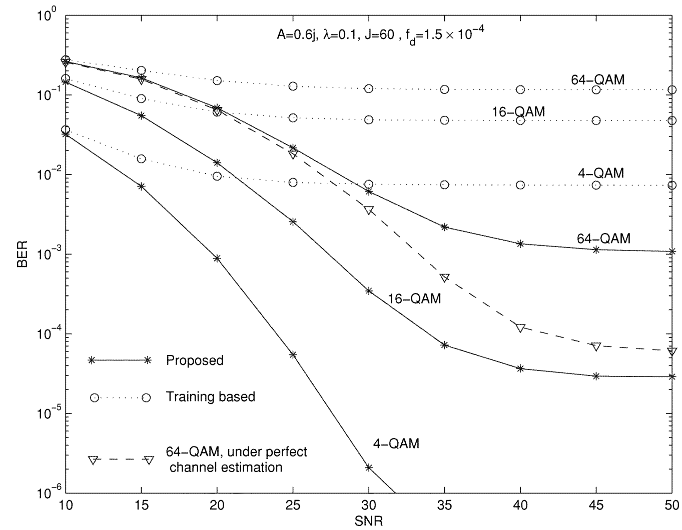

Fig. 4. BER performance of the proposed approach and the training-based method. Ideal value of BER for 64-QAM, when the channel is perfectly known, for proposed approach is shown by dashed/triangle line.

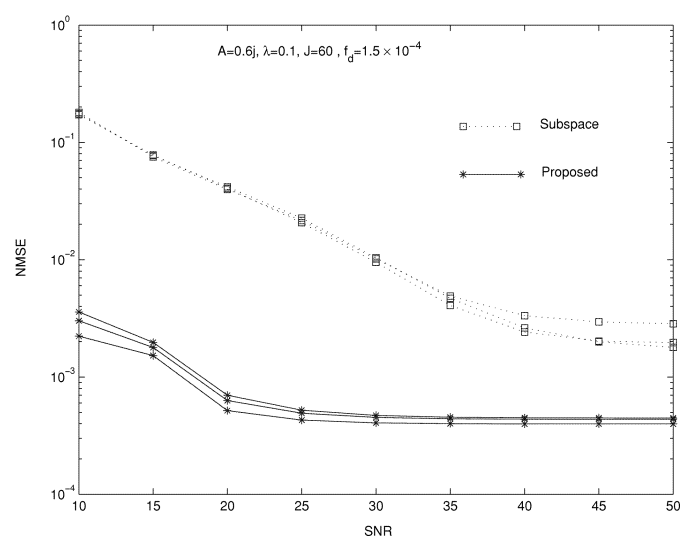

Fig. 5. Fast-varying channel: NMSE of proposed approach and that of the blind subspace method of [27].

The BER performance of the subspace method of [27] is also shown in Fig. 2(b), obtained based on the same parameters used for the proposed method. It can be seen that it is comparable to that of the training method and slightly better than the proposed. It should be noted though that the complexity of the subspace approach is significantly higher as it is based on singular value decomposition of the autocorrelation matrix.

B. *Fast-Varying Channel*

Next, we consider the case of a fast-varying channel with $f_d = 1.5 \times 10^{-4}$ and simulated transmission of $N_s = 600$ OFDM symbols. Fig. 3(a) shows the NMSE_{i_0} versus i_0, for the proposed and training-based methods, at $\mathrm{SNR} = 20$ dB. Here, averaging was performed over $J = 60$ blocks, and we took $\lambda = 0.1$ and $A = j0.6$. The minimum channel gain was -16.5 dB. The average NMSE is shown in Fig. 3(b) as a function of the SNR, while the corresponding BER is shown in Fig. 4. As it can be seen from Figs. 3 and 4, the proposed blind channel estimation approach not only achieves lower channel error than the training-based one, but also results in lower BER. This behavior suggests that 600 blocks is too long for the channel to be assumed constant [which can also be seen from Fig. 3(a)] and that the training method would have to use additional training data in order to guarantee low BER.

On the other hand, the proposed method tracks the channel very well. To get an idea of how much the channel errors affect the BER, we also provide in Fig. 4 the BER of 64-QAM corresponding to the proposed approach operating under perfect channel estimation.

Figs. 5 and 6 compare the performance of the subspace method of [27] against the proposed one for the fast-varying channels based on $N_s = 520$ OFDM symbols, $\lambda = 0.1$, and smoothing factor $J = 130$. The value of A is still $j0.6$ as above.

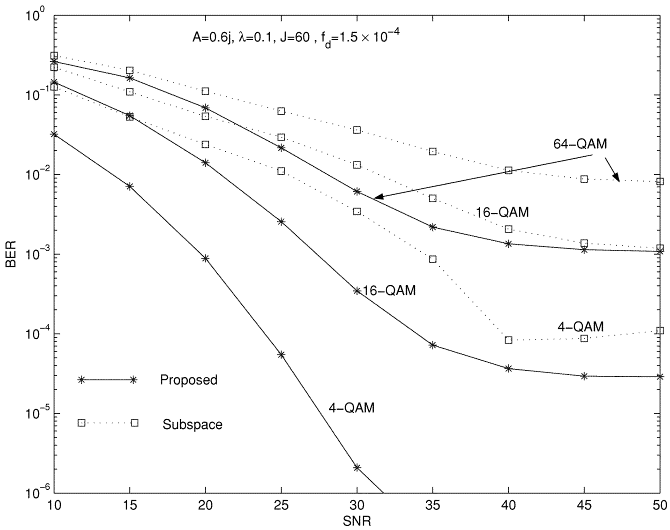

Fig. 6. BER performance of the proposed approach and that of the blind subspace method of [27].

One can see that the proposed approach outperforms the subspace method. It should also be noted that the performance of the subspace method could not be improved by decreasing the smoothing factor in anticipation of the fast-varying channel. In theory, it requires a smoothing factor of at least twice the block length (i.e., $J = 128$). Our simulations actually suggested that J had to be greater than 130 for the method to produce meaningful results even for slowly varying channels.

VI. Conclusion

We propose a computationally simple approach for blind channel estimation in OFDM systems. At the transmitter, a simple preprocessing is performed at each block, which induces correlation structure to the block. This structure is exploited at the receiver to estimate the channel within a complex scalar. Simulations showed that the proposed method compares favorably to training-based and subspace approaches.

Although it might appear that adding a constant to the block during the precoding step would result is a simpler channel estimation method that would employ first-order statistics of the received signal, such an approach would introduce a bias to each carrier. Such a bias is not desirable in a practical system. The proposed precoding maintains the zero-mean of each carrier.

Appendix

A. Proof of (12)

It is convenient to use matrix representations. The following notation is used for special matrices and operations:

- $\boldsymbol{u}$ — $N \times 1$ vector with 1 at even indexed entries and -1 at the odd indexed entries;
- e_n — $N \times 1$ vector with 1 at the nth entry and 0 at others;
- $\boldsymbol{I}_n$ — $n \times n$ identity matrix;
- $\boldsymbol{F}$ — $N \times L$ matrix composed of the first L columns of an $N \times N$ DFT matrix, the (k,l)th element being $e^{-j(2\pi/N)kl}$;
- $(\cdot)'$ — matrix for vector transpose;
- $(\cdot)^*$ — matrix, vector, or scalar conjugate;
- $\mathcal{D}(\boldsymbol{x})$ — diagonal matrix with the elements of the vector x on the diagonal.

We also define

$$\begin{aligned}\boldsymbol{y_i} &\triangleq \left[y_{i,0}, \dots, y_{i,(N-1)}\right]'\\ \boldsymbol{d_i} &\triangleq \left[d_{i,0}, \dots, d_{i,(N-1)}\right]'\\ \boldsymbol{v_i} &\triangleq \left[v_{i,0}, \dots, v_{i,(N-1)}\right]'\\ \tilde{\boldsymbol{h}} &\triangleq [H(0), \dots, H(N-1)]'.\end{aligned}$$

With the above conventions, we rewrite (2) in matrix form as

$$\boldsymbol{y}_i = \mathcal{D}(\tilde{\boldsymbol{h}})\mathcal{D}(\boldsymbol{a})(\boldsymbol{d}_i + Ad_{i,T}\boldsymbol{u}) + \boldsymbol{v}_i \tag{A.1}$$

where $\boldsymbol{a}$ is an $N \times 1$ vector with $1/\sqrt{1+|A|^2}$ at each entry. The channel estimate obtained using the proposed method and based on finite (J) samples can be expressed as [cf. (4)]

$$\hat{\tilde{\boldsymbol{h}}} = \mathcal{D}(\boldsymbol{b})\left(\frac{1}{J}\sum_{i=1}^{J}\boldsymbol{y}_i y_{i,T}^*\right) \tag{A.2}$$

where $\boldsymbol{b}$ is an $N \times 1$ vector with 1 at the Tth entry and $(1+|A|^2/(-1)^k A + (-1)^{k+T}|A|^2)$ at the kth entry. From (A.2), we have

$$\mathrm{E}[\hat{\tilde{\boldsymbol{h}}}] = \sigma_d^2 H^*(T)\tilde{\boldsymbol{h}} + \sigma_v^2 \boldsymbol{e}_T. \tag{A.3}$$

The improvement of channel estimate by enforcing the channel memory length at time-domain can be described as [cf.(5)]

$$\hat{\tilde{\boldsymbol{h}}}_o = \frac{1}{N}\boldsymbol{F}\boldsymbol{F}^{*\prime}\hat{\tilde{\boldsymbol{h}}}. \tag{A.4}$$

Consequently, the NMSE defined in (11) becomes (A.5), as shown at the bottom of the page. Using (A.2) and

$$\begin{aligned}\mathrm{NMSE} &= \frac{\mathrm{E}\left[\left\|\frac{\hat{\tilde{\boldsymbol{h}}}_o}{\sigma_d^2 H^*(T)} - \tilde{\boldsymbol{h}}\right\|^2\right]}{\|\tilde{\boldsymbol{h}}\|^2} = \frac{\mathrm{E}\left[\left(\frac{\hat{\tilde{\boldsymbol{h}}}}{\sigma_d^2 H^*(T)} - \tilde{\boldsymbol{h}}\right)^{*\prime}\boldsymbol{F}\boldsymbol{F}^{*\prime}\left(\frac{\hat{\tilde{\boldsymbol{h}}}}{\sigma_d^2 H^*(T)} - \tilde{\boldsymbol{h}}\right)\right]}{N\|\tilde{\boldsymbol{h}}\|^2}\\ &= \frac{\mathrm{trace}\left\{\boldsymbol{F}^{*\prime}\mathrm{E}\left[\left(\frac{\hat{\tilde{\boldsymbol{h}}}}{\sigma_d^2 H^*(T)} - \tilde{\boldsymbol{h}}\right)\left(\frac{\hat{\tilde{\boldsymbol{h}}}}{2\sigma_d^2 H^*(T)} - \tilde{\boldsymbol{h}}\right)^{*\prime}\right]\boldsymbol{F}\right\}}{N\|\tilde{\boldsymbol{h}}\|^2}\end{aligned} \tag{A.5}$$

$$\begin{aligned}
&\mathrm{E}\left[\left(\frac{\hat{\tilde{\boldsymbol{h}}}}{\sigma_d^2 H^*(T)}-\tilde{\boldsymbol{h}}\right)\left(\frac{\hat{\tilde{\boldsymbol{h}}}}{\sigma_d^2 H^*(T)}-\tilde{\boldsymbol{h}}\right)^{*\prime}\right]\\
&=\frac{\mathrm{E}\left[\left(\hat{\tilde{\boldsymbol{h}}}-\mathrm{E}[\hat{\tilde{\boldsymbol{h}}}]-\sigma_v^2\boldsymbol{e}_T\right)\left(\hat{\tilde{\boldsymbol{h}}}-\mathrm{E}[\hat{\tilde{\boldsymbol{h}}}]-\sigma_v^2\boldsymbol{e}_T\right)^{*\prime}\right]}{\sigma_d^4|H(T)|^2}\\
&=\frac{\mathrm{E}\left[\left(\hat{\tilde{\boldsymbol{h}}}-\mathrm{E}[\hat{\tilde{\boldsymbol{h}}}]\right)\left(\hat{\tilde{\boldsymbol{h}}}-\mathrm{E}[\hat{\tilde{\boldsymbol{h}}}]\right)^{*\prime}\right]}{\sigma_d^4|H(T)|^2}+\frac{\sigma_v^4\boldsymbol{e}_T\boldsymbol{e}_T'}{\sigma_d^4|H(T)|^2}\\
&=\frac{\mathcal{D}(\boldsymbol{b})\mathrm{E}\left[\sum_{i=1}^J\left(\boldsymbol{y}_i y_{i,T}^*-\mathrm{E}[\boldsymbol{y}_i y_{i,T}^*]\right)\sum_{i=1}^J\left(\boldsymbol{y}_i y_{i,T}^*-\mathrm{E}[\boldsymbol{y}_i y_{i,T}^*]\right)^{*\prime}\right]\mathcal{D}(\boldsymbol{b}^*)}{J^2\sigma_d^4|H(T)|^2}+\frac{\sigma_v^4\boldsymbol{e}_T\boldsymbol{e}_T'}{\sigma_d^4|H(T)|^2}\\
&=\frac{\mathcal{D}(\boldsymbol{b})\sum_{i=1}^J\sum_{j=1}^J\mathrm{E}\left[\left(\boldsymbol{y}_i y_{i,T}^*-\mathrm{E}[\boldsymbol{y}_i y_{i,T}^*]\right)\left(\boldsymbol{y}_j y_{j,T}^*-\mathrm{E}[\boldsymbol{y}_j y_{j,T}^*]\right)^{*\prime}\right]\mathcal{D}(\boldsymbol{b}^*)}{J^2\sigma_d^4|H(T)|^2}+\frac{\sigma_v^4\boldsymbol{e}_T\boldsymbol{e}_T'}{\sigma_d^4|H(T)|^2}\\
&=\frac{\mathcal{D}(\boldsymbol{b})\left(\mathrm{E}\left[\boldsymbol{y}_i\boldsymbol{y}_i^{*\prime}y_{i,T}y_{i,T}^*\right]-\mathrm{E}\left[\boldsymbol{y}_i y_{i,T}^*\right]\mathrm{E}\left[\boldsymbol{y}_i^{*\prime}y_{i,T}\right]\right)\mathcal{D}(\boldsymbol{b}^*)}{J\sigma_d^4|H(T)|^2}+\frac{\sigma_v^4\boldsymbol{e}_T\boldsymbol{e}_T'}{\sigma_d^4|H(T)|^2}\\
&=\frac{\mathcal{D}(\boldsymbol{b})\mathrm{E}\left[\boldsymbol{y}_i\boldsymbol{y}_i^{*\prime}y_{i,T}y_{i,T}^*\right]\mathcal{D}(\boldsymbol{b}^*)}{J\sigma_d^4|H(T)|^2}\\
&\quad-\frac{1}{J}\left[\tilde{\boldsymbol{h}}\tilde{\boldsymbol{h}}^{*\prime}+\frac{\sigma_v^2}{\sigma_d^2H(T)}\tilde{\boldsymbol{h}}\boldsymbol{e}_T'+\frac{\sigma_v^2}{\sigma_d^2H^*(T)}\boldsymbol{e}_T\tilde{\boldsymbol{h}}^{*\prime}+\frac{\sigma_v^4}{\sigma_d^4|H(T)|^2}\boldsymbol{e}_T\boldsymbol{e}_T'\right]+\frac{\sigma_v^4\boldsymbol{e}_T\boldsymbol{e}_T'}{\sigma_d^4|H(T)|^2}
\end{aligned}\tag{A.6}$$

(A.3), we obtain (A.6), shown at the top of the page. Furthermore

$$\begin{aligned}
&\mathrm{E}\left[\boldsymbol{y}_i\boldsymbol{y}_i^{*\prime}y_{i,T}y_{i,T}^*\right]\\
&=|H(T)|^2\mathcal{D}(\tilde{\boldsymbol{h}})\mathcal{D}(\boldsymbol{a})\mathrm{E}\\
&\quad\times\left[(\boldsymbol{d}_i+Ad_{i,T}\boldsymbol{u})(\boldsymbol{d}_i+Ad_{i,T}\boldsymbol{u})^{*\prime}|d_{i,T}|^2\right]\mathcal{D}(\boldsymbol{a}^*)\mathcal{D}(\tilde{\boldsymbol{h}}^*)\\
&\quad+\mathcal{D}(\tilde{\boldsymbol{h}})\mathcal{D}(\boldsymbol{a})\mathrm{E}\left[(\boldsymbol{d}_i+Ad_{i,T}\boldsymbol{u})(\boldsymbol{d}_i+Ad_{i,T}\boldsymbol{u})^{*\prime}\right]\\
&\quad\times\mathrm{E}\left[|v_{i,T}|^2\right]\mathcal{D}(\boldsymbol{a}^*)\mathcal{D}(\tilde{\boldsymbol{h}}^*)\\
&\quad+\frac{1+(-1)^TA^*}{\sqrt{1+|A|^2}}H^*(T)\mathcal{D}(\tilde{\boldsymbol{h}})\mathcal{D}(\boldsymbol{a})\\
&\quad\times\mathrm{E}\left[(\boldsymbol{d}_i+Ad_{i,T}\boldsymbol{u})d_{i,T}^*\right]\mathrm{E}\left[\boldsymbol{v}_i^{*\prime}v_{i,T}\right]\\
&\quad+\frac{1+(-1)^TA}{\sqrt{1+|A|^2}}H(T)\mathrm{E}\left[v_{i,t}^*\boldsymbol{v}_i\right]\\
&\quad\times\mathrm{E}\left[d_{i,T}(\boldsymbol{d}_i+Ad_{i,T}\boldsymbol{u})^{*\prime}\right]\\
&\quad\times\mathcal{D}(\boldsymbol{a}^*)\mathcal{D}(\tilde{\boldsymbol{h}}^*)\\
&\quad+|H(T)|^2\mathrm{E}\left[|d_{i,t}|^2\right]\mathrm{E}\left[\boldsymbol{v}_i\boldsymbol{v}_i^{*\prime}\right]\\
&\quad+\mathrm{E}\left[\boldsymbol{v}_i\boldsymbol{v}_i^{*\prime}|v_{i,t}|^2\right]\\
&=\sigma_d^4|H(T)|^2\mathcal{D}(\tilde{\boldsymbol{h}})\mathcal{D}(\boldsymbol{a})(\boldsymbol{I}_N-\boldsymbol{e}_T\boldsymbol{e}_T')\mathcal{D}(\boldsymbol{a}^*)\mathcal{D}(\tilde{\boldsymbol{h}}^*)\\
&\quad+\psi_4|H(T)|^2\mathcal{D}(\tilde{\boldsymbol{h}})\mathcal{D}(\boldsymbol{a})(\boldsymbol{e}_T+A\boldsymbol{u})\\
&\quad\times(\boldsymbol{e}_T+A\boldsymbol{u})^{*\prime}\mathcal{D}(\boldsymbol{a}^*)\mathcal{D}(\tilde{\boldsymbol{h}}^*)\\
&\quad+\sigma_v^2\sigma_d^2\mathcal{D}(\tilde{\boldsymbol{h}})\mathcal{D}(\boldsymbol{a})(\boldsymbol{I}_N-\boldsymbol{e}_T\boldsymbol{e}_T')\mathcal{D}(\boldsymbol{a}^*)\mathcal{D}(\tilde{\boldsymbol{h}}^*)\\
&\quad+\sigma_v^2\sigma_d^2\mathcal{D}(\tilde{\boldsymbol{h}})\mathcal{D}(\boldsymbol{a})(\boldsymbol{e}_T+A\boldsymbol{u})(\boldsymbol{e}_T+A\boldsymbol{u})^{*\prime}\mathcal{D}(\boldsymbol{a}^*)\mathcal{D}(\tilde{\boldsymbol{h}}^*)\\
&\quad+\frac{1+(-1)^TA^*}{\sqrt{1+|A|^2}}\sigma_v^2\sigma_d^2H^*(T)\mathcal{D}(\tilde{\boldsymbol{h}})\mathcal{D}(\boldsymbol{a})(\boldsymbol{e}_T+A\boldsymbol{u})e_T'\\
&\quad+\frac{1+(-1)^TA}{\sqrt{1+|A|^2}}\sigma_v^2\sigma_d^2H(T)e_T(\boldsymbol{e}_T+A\boldsymbol{u})'\mathcal{D}(\boldsymbol{a}^*)\mathcal{D}(\tilde{\boldsymbol{h}}^*)\\
&\quad+\sigma_v^2\sigma_d^2|H(T)|^2\boldsymbol{I}_N\\
&\quad+\sigma_v^4(\boldsymbol{I}_N+\boldsymbol{e}_T\boldsymbol{e}_T').
\end{aligned}\tag{A.7}$$

Substituting (A.7) into (A.6) and then into (A.5), the desired result of (12) follows.

REFERENCES

[1] *The DWMT: A Multicarrier Transceiver for ADSL Using M-Band Wavelets ANSI Standard*, 1993.

[2] "Broadband Radio Access Networks (BRAN): HIPERLAN Type 2 technical specifications Part 1—Physical layer ETSI DTS/ BRAN030 003–1,", 1999.

[3] *Digital Video Broadcasting: Framing Structure, Channel Coding and Modulation for Digital Terrestrial Television European Telecommunications Standard*, 1997.

[4] *Radio Boadting Systems: Digital Audio Broadcasting to Mobile, Portable and Fixed Receivers Eurpoean Telecommunications Standard*, 1995.

[5] *Wireless LAN Medium Access Control (MAC) and Physical Layer (PHY) Specifications IEEE Standard 802.11a, Part 11*, 1999.

[6] A. Akansu, P. Duhamel, X. Lin, and M. De Courville, "Orthogonal transmultiplexers in communications: A review," *IEEE Trans. Signal Processing*, vol. 463, pp. 979–995, Apr. 1998.

[7] H. Ali, J. H. Manton, and Y. Hua, "A sos subspace method for blind channel identification and equalization in bandwidth efficient ofdm systems based on receive antenna diversity," in *Proc. SSAP*, Singapore, Aug. 2001, pp. 401–404.

[8] J. van de Beek, O. Edfors, M. Sandell, S. K. Wilson, and P. O. Böjesson, "On channel estimation in OFDM system," in *Proc. Vehicle Technology Conf.*, vol. 2, Chicago, IL, July 1995, pp. 815–819.

[9] J. A. C. Bingham, "Multicarrier modulation for data transmission: An idea whose time has come," *IEEE Commun. Mag.*, May 1990.

[10] R. S. Blum, Y. Li, J. H. Winters, and Q. Yan, "Improved space-time coding for MIMO-OFDM wireless communictions," *IEEE Trans. Commun.*, vol. 49, pp. 1873–1878, Nov. 2001.

[11] X. Cai and A. N. Akansu, "A subspace method for blind channel identification in OFDM systems," in *Proc. ICC*, New Orleans, LA, July 2000, pp. 929–933.

[12] N. Chotikakamthorn and H. B. Suzuki, "On identifiablility of OFDM blind channel estimation," in *Proc. VTC*, Amsterdam, The Netherlands, Sept. 1999, pp. 2358–2361.
[13] L. J. Cimini Jr, "Analysis and simulation of a digital mobile channel using orthogonal frequency division multiplexing," *IEEE Trans. Commun.*, vol. 33, pp. 665–675, July 1985.
[14] O. Edfors, M. Sandell, J.-J. van de Beek, S. K. Wilson, and P. O. Böjesson, "OFDM channel estimation by singular value decomposition," *IEEE Trans. Commun.*, vol. 46, pp. 931–939, July 1998.
[15] G. B. Giannakis, "Filterbanks for blind channel identification and equalization," *IEEE Trans. Signal Processing*, vol. 4, pp. 184–187, June 1997.
[16] R. W. Heath and G. B. Giannakis, "Exploiting input cyclostationarity for blind channel identification in OFDM systems," *IEEE Trans. Signal Processing*, vol. 47, pp. 848–856, Mar. 1999.
[17] Y. R. Zheng and C. Xiao, "Improved models for the generation of multiple uncorrelated Rayleigh fading waveforms," *IEEE Commun. Lett.*, vol. 6, pp. 256–258, June 2002.
[18] Y. Li, "Pilot-symbol-aided channel estimation for OFDM in wireless systems," *IEEE Trans. Veh. Technol.*, vol. 48, pp. 1207–1215, July 2000.
[19] ——, "Simplified channel estimation for OFDM systems with multiple transmit antennas," *IEEE Trans. Wireless Commun.*, vol. 1, pp. 67–75, Jan. 2002.
[20] Y. Li, L. J. Cimini Jr, and N. R. Sollengerger, "Robust channel estimation for OFDM systems with rapid dispersive fading channels," *IEEE Trans. Commun.*, vol. 46, pp. 902–915, Jul. 1998.
[21] Y. Li, N. Seshadri, and S. Ariyavisitakul, "Channel estimation for OFDM systems with transmitter diversity in mobile wireless channels," *IEEE J. Select. Areas Commun.*, vol. 17, pp. 461–471, Mar. 1999.
[22] L. Lin, J. C.-I. Chuang, and Y. Li, "Near optimal joint channel estimation and data detection for COFDM systems," in *Proc. Globalcomm*, San Francisco, CA, Nov. 2000.
[23] B. Lu and X. Wang, "Bayesian blind turbo receiver for coded OFDM systems with frequency offset and frequency-selective fading," *IEEE J. Select. Areas Commun.*, vol. 19, pp. 2516–2527, Dec. 2001.
[24] B. Lu, X. Wang, and K. R. Narayanan, "LDPC-based spacetime coded OFDM systems over correlated fading channels: Analysis and receiver design," *IEEE Trans. Commun.*, vol. 50, pp. 74–88, Jan. 2002.
[25] B. Lu, X. Wang, and Y. G. Li, "Iterative receivers for space-time block coded OFDM systems in fading channels," *IEEE Trans. Wireless Commun.*, vol. 1, pp. 213–225, Apr. 2002.
[26] M. Morelli and U. Mengali, "A comparison of pilot-aided channel estimation methods for OFDM systems," *IEEE Trans. Signal Processing*, vol. 49, pp. 3065–3073, Dec. 2001.
[27] B. Muquet, M. de Courville, and P. Duhamel, "Subspace-based blind and semi-blind channel estimation for OFDM systems," *IEEE Trans. Signal Processing*, vol. 50, pp. 1699–1712, July 2002.
[28] H. Wang, Y. Lin, and B. Chen, "Blind OFDM channel estimation using receiver diversity," in Proc. Conf. Information Science Systems, Princeton, NJ, Mar. 2002.
[29] Z. Yang and G. B. Giannakis, "Wireless multicarrier communications: Where Fourier meets shannon," *IEEE Signal Processing Mag.*, pp. 29–48, May 2000.
[30] Z. Yang and X. Wang, "Blind detection of OFDM signals in multipath fading channels via sequential Monte Carlo," *IEEE Trans. Signal Processing*, vol. 50, pp. 255–270, Feb. 2002.
[31] S. Zhou and G. B. Giannakis, "Finite-Alphabet based channel estimation for OFDM and related multicarrier systems," *IEEE Trans. Commun.*, vol. 49, pp. 1402–1414, Aug. 2001.
[32] X. Zhuang, Z. Ding, and A. L. Swindlehurst, "A statistical subspace method for blind channel identification in OFDM communications," in *Proc. ICASSP*, vol. 5, Istanbul, Turkey, June 2000, pp. 2493–2496.

Athina Petropulu received the Diploma in electrical engineering from the National Technical University of Athens, Greece, in 1986 and the M.Sc. degree in electrical and computer engineering in 1988, and the Ph.D. degree in electrical and computer engineering in 1991, both from Northeastern University, Boston, MA.

In 1992, she joined the Department of Electrical and Computer Engineering, Drexel University, Philadelphia, PA, where she is now a Professor. During the academic year 1999/2000 she was an Associate Professor at Université Paris Sud, École Supérieure d'Electricité, Paris, France. Her research interests include the area of statistical signal processing, communications, higher order statistics, fractional-order statistics, and ultrasound imaging. She is the co-author of the textbook entitled *Higher-Order Spectra Analysis: A Nonlinear Signal Processing Framework* (Englewood Cliffs, NJ: Prentice-Hall, 1993).

Dr. Petropulu is the recipient of the 1995 Presidential Faculty Fellow Award. She has served as an Associate Editor for the IEEE TRANSACTIONS ON SIGNAL PROCESSING and the IEEE SIGNAL PROCESSING LETTERS. She is a member-at-large of the IEEE Signal Processing Board of Governors and a member of the IEEE Signal Processing Society Conference Board and the Technical Committee on Signal Processing Theory and Methods. She is the general chair of the 2005 IEEE International Conference on Acoustics, Speech, and Signal Processing (ICASSP).

Ruifeng Zhang (M'97) received the B.S. degree from Huazhong University of Science and Technology, Wuhan, China, in 1993, the M.E. degree from Beijing Institute of Technology, Beijing, China, in 1996, and the Ph.D. degree from Stevens Institute of Technology, Hoboken, NJ, all in electrical engineering.

He is an Assistant Professor of the Electrical and Computer Engineering Department, Drexel University, Philadelphia, PA, which he joined in 2000. He was a Postdoctoral Associate and Research Assistant at the Electrical and Computer Engineering Department, Stevens Institute of Technology from 1997 to 2000. His research interests include the areas of statistical signal processing and communications. The current focus of his work is on signal processing methods for wireless networks.

Dr. Zhang has been Chair of the joint SP/BT/CE Chapter, IEEE Philadelphia Section since 2001. He serves on the organizing committee for the 2005 ICASSP. He was a recipient of the 2002 IEEE SP Society Best Paper Award. He also received the Peskin Award from Stevens Institute of Technology in 2000 and AT&T and the ACM Student Research Award in 1999.

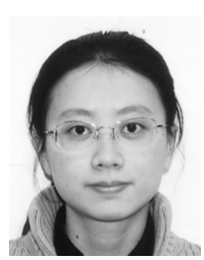

Rui Lin was born in China in 1975. She received the B.S. degree in 1997 and the M.Sc. degree in 2000 from the Huazhong University of Science and Technology, Wuhan, China, both in electrical engineering. She is currently working toward the Ph.D. degree at Drexel University, Philadelphia PA.

Her research interests include the areas of communications and signal processing, including blind channel estimation and equalization algorithms and wireless, multicarrier, spread-spectrum communication systems.